NASA TECHNICAL NOTE
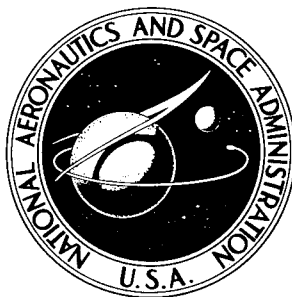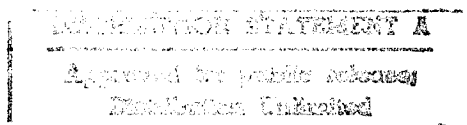
NASA TN D-3486

19960419 043

ANALYTICAL DETERMINATION OF THE EFFECT OF THERMAL PROPERTY VARIATIONS ON THE PERFORMANCE OF A CHARRING ABLATOR

by Claud M. Pittman and William D. Brewer

Langley Research Center
Langley Station, Hampton, Va.

DTIC QUALITY INSPECTED 1

DISCLAIMER NOTICE

THIS DOCUMENT IS BEST
QUALITY AVAILABLE. THE
COPY FURNISHED TO DTIC
CONTAINED A SIGNIFICANT
NUMBER OF PAGES WHICH DO
NOT REPRODUCE LEGIBLY.

ANALYTICAL DETERMINATION OF THE EFFECT

OF THERMAL PROPERTY VARIATIONS ON THE

PERFORMANCE OF A CHARRING ABLATOR

By Claud M. Pittman and William D. Brewer

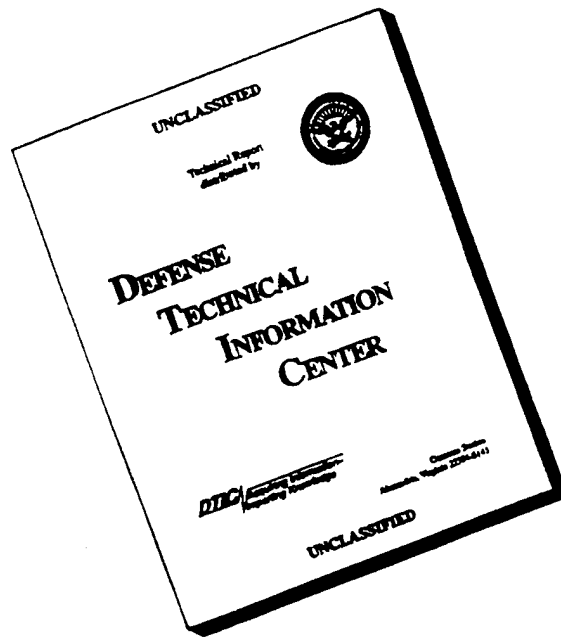Langley Research Center
Langley Station, Hampton, Va.

NATIONAL AERONAUTICS AND SPACE ADMINISTRATION

ANALYTICAL DETERMINATION OF THE EFFECT

OF THERMAL PROPERTY VARIATIONS ON THE

PERFORMANCE OF A CHARRING ABLATOR

By Claud M. Pittman and William D. Brewer
Langley Research Center

SUMMARY

An analytical investigation of the effects of varying certain material properties on the performance of a charring ablator material has been made. The quantities which are varied are char conductivity, conductivity and specific heat of the uncharred material, heat of pyrolysis, temperature of pyrolysis, and the specific heat of the gases of pyrolysis. The effects of these variations on surface recession, charred-uncharred interface recession, and internal temperature histories are shown. The analytical results are compared with experimental results and representative material property values are found which provide good agreement.

INTRODUCTION

Vehicles entering the earth's atmosphere at high velocities are subjected to severe heating. A number of methods are available for protecting the interior of a reentering spacecraft. In general, charring ablators, subliming ablators, and melting ablators provide the most effective thermal protection systems. Of these, the charring ablator is superior for a wide range of applications including the stagnation area of manned reentry vehicles. (See ref. 1.)

It is necessary to be able to predict the performance of ablation materials in reentry environments in order to design efficient and reliable thermal protection systems for flight vehicles. Some flight tests have been proposed to determine the performance of certain charring ablator materials in the reentry environment. However, flight tests are both expensive and time-consuming and it is hardly practical to test all the promising charring ablator materials in this manner.

Several computer programs have been formulated with which the performance of a thermal protection material in a heating environment can be predicted. One such computer program has been developed at the Langley Research Center and is described in reference 2. However, many of the input quantities that are required to obtain a solution with

this program are not well established. For example, very little data are available on the specific heat of the gaseous products of pyrolysis. There are some data available on the thermal conductivity of the char layer at high temperatures; however, there is considerable disagreement in these data among the various references. (See, for example, refs. 3 and 4.) The main reason for the lack of data and the wide scatter in the available data is the extremely complicated physical and chemical changes which take place in a degrading charring ablator. It is very possible that none of the presently used techniques for obtaining data (usually involving steady-state measurements) give material property values which are representative of the actual values in the dynamic degradation process.

This paper presents the results of an analytical investigation conducted to determine the effect of varying certain material property values on the performance of a charring ablator in a heating environment. The quantities which were varied in the calculations were as follows: the thermal conductivity of the char, the specific heat and thermal conductivity of the uncharred material, the heat of pyrolysis, the temperature of pyrolysis and the specific heat of the gases of pyrolysis. The analytical results are compared with experimental test results to determine whether the values of the properties used in the calculations are representative of the actual values for the material. An attempt is made to determine more nearly correct values of material properties by varying them in the calculation to obtain agreement between experimental and analytical results.

SYMBOLS

The units used for the quantities defined in this paper are given both in the U.S. Customary Units and in the International System of Units (SI). Factors relating the two systems are given in reference 5.

A, B, C   constants

c_p specific heat

$\bar{c}_p$ specific heat of gases of pyrolysis

Δh heat of pyrolysis

k   thermal conductivity

$\dot{m}$ mass loss rate

2

T	temperature
$\bar{T}$	temperature of pyrolysis

Subscripts:

c	char
o	uncharred material
s	standard

ANALYTICAL PROGRAM AND PROCEDURE

Basic Program

The equations derived in reference 2 provide a means for predicting the behavior of a thermal protection system in any heating environment. The accuracy of the results obtained depends mainly on the precision with which the heating environment and properties of the materials are known.

The equations were derived primarily to provide a means for investigating the performance of charring ablators. However, the same equations are suitable for the analysis of other thermal protection systems.

Procedure

The analysis of reference 2 is designed to yield temperature distributions and dimensional changes as functions of time. To obtain these results, it is necessary to specify certain environmental and material properties.

The environmental parameters necessary for the analysis are the enthalpy of the test stream, the heating rate to the material, and the composition of the test stream. It was assumed that these quantities could be measured with sufficient accuracy that they were not considered variables in the analytical inputs.

Data for many of the material property values for the material tested are not available at the present time. This fact is especially true of those properties which are strong functions of temperature. Although room-temperature measurements have been made for several properties, and thus provide a base for the variation, values at higher temperatures are not available.

A calculation was made in which representative material property values were used, and this calculation is referred to as the standard. Temperatures within the material, the surface recession, and the recession of the interface between the char and uncharred material obtained from the standard calculation were compared with those obtained experimentally. Because of the disagreement between the experimental and calculated results, and in view of the uncertainties in the material properties, calculations were made by varying one property at a time and the results were compared with the standard calculation. With this procedure the effect of varying each material property on the performance of the material could be determined. After the results of the various calculations and the comparison of the calculated and experimental results were considered, the material properties were changed in such a manner to give analytical results which were in closer agreement with the experimental results.

Because of the great number of material property inputs, it was desirable to assume that the values and variations of as many of these inputs as possible were known well enough to be considered as fixed quantities for all the calculations. In this investigation, the quantities which were considered fixed were the density and specific heat of the char, the emissivity of the char surface, and the density of the virgin material. The quantities which were varied in the calculations were as follows: the thermal conductivity of the char, the specific heat and thermal conductivity of the uncharred material, the heat of pyrolysis, the temperature of pyrolysis, and the specific heat of the gases of pyrolysis.

EXPERIMENTAL TEST SPECIMENS AND PROCEDURES

Test Specimens

The material used in this test program was an epoxy base material filled with phenolic Microballoons (20 percent) and silica fibers (20 percent). The nominal density of the material was 57.5 pounds per cubic foot (920 kg/m^3).

The specimens were supplied in the form of 3-inch (7.6-cm) diameter, flat-faced disks. The thicknesses varied from 5/8 to $1\frac{1}{4}$ inches (1.6 to 3.2 cm). A brass mounting ring was bonded to the back surface of each specimen to allow positioning of the specimen on the test apparatus.

In general, two types of specimens were tested. One type had no instrumentation and is referred to as an uninstrumented specimen. The other type of specimen had thermocouples located at various depths in the material and is referred to as an instrumented specimen. Each instrumented specimen also had a thermocouple attached to its back surface so that the back surface temperature could be monitored during the tests. All thermocouples were platinum—platinum-13-percent-rhodium made from No. 24 gage wire.

A typical thermocouple installation for the instrumented specimen is shown in figure 1. The thermocouple junction was formed by butt-welding two single wires. The wires were positioned in a hole lying along a diameter of the specimen so that the junction was located on the vertical axis of the specimen, and then cemented in place. From the junction, the wires extended radially outward in opposite directions and back through ceramic tubing cemented in grooves along the side of the specimen. The thermocouple junctions were located approximately 1/8 inch apart (measured along the vertical axis of the specimen). A photograph of one of the instrumented specimens prior to attaching the mounting ring is shown in figure 2.

Test Conditions and Procedures

All specimens were tested in the Langley 2500-kilowatt arc jet. This facility produces a subsonic (Mach number ≈ 0.9) gas stream at atmospheric pressure with a static temperature of about 7200° R (4000° K). The facility is described in detail in reference 6. The test conditions are summarized in table I. The particular heating rates and enthalpy shown in the table were used because they are the values obtained at the normal operating conditions of the arc-jet facility. The heating rates were determined by the use of a 3-inch (7.6-cm) diameter, flat-faced, thin metallic calorimeter. The calorimeter was inserted into the test stream before each test. The test specimens were inserted into the test stream immediately after removing the calorimeter. One series of tests was made with a test-stream composition of 5-percent oxygen and 95-percent nitrogen. This composition was used because, as shown in reference 7, the char performance in flight environments is adequately simulated in low-enthalpy test facilities only if the oxygen content of the test stream is reduced. A test stream of 100-percent nitrogen was used in a second series of tests to compare results in two different heating environments.

Uninstrumented specimens were tested to determine the movement of the front surface and the interface. To accomplish this, specimens were tested at the same conditions for the times indicated in table I. The specimens were then sectioned and the locations of the front surface and the interface were determined.

The instrumented specimens were tested until a back surface temperature rise of 300° R (167° K) was observed. The purpose of these tests was to determine temperature histories within the material.

RESULTS AND DISCUSSION

The results of this investigation are given in figures 3 to 12. The input values used for the standard case, the variations used for the more uncertain properties, and the final property values which give the best agreement with experimental results are given in

table II. Comparisons of the final case and the experimental results for both environments considered are shown in figures 10 and 12. The numbers at the top of the temperature curves indicate the thermocouple depths from the original front surface.

Standard Case

The input values used for the standard calculation are given in table II. The variation of char conductivity with temperature for the standard case is of the form

$$k_c = AT^3 - BT + C$$

where k_c is the thermal conductivity of the char; A, B, and C are constants; and T is the temperature in °R.

This form was chosen so that at low temperatures when conduction is the primary means of heat transfer, the T term is significant and at high temperatures, when most of the heat is transferred by radiation within the pores, the T^3 term is dominant. Since the program discussed previously requires an analytical model which consists of at least two primary layers, the calculations must begin with a finite char thickness and, as a result, the thermal protection due to mass transfer in forming the small initial char layer is neglected. The values of the conductivity at low temperatures were made low to compensate for this neglected protection. The char conductivity used in the standard case is in reasonable agreement with the values given in reference 3.

From the densities of the char and the uncharred material, which are fairly easily obtained, and the composition of the original material, it was deduced that the char should be about half carbon and half quartz. The specific heat of the char used in all cases is therefore the average of the specific heats of the two constituents.

The values for the thermal conductivity and the specific heat of the uncharred material, the heat of pyrolysis, and the temperature of pyrolysis are approximate values obtained from the manufacturer of the ablation material. The dependence of these properties upon temperature is not known.

The specific heat of the gases of pyrolysis used in the standard case increased linearly with temperature. This choice of variation is arbitrary since very little information is available concerning the gases of pyrolysis.

A comparison of the results of the standard calculation with the experimental data is shown in figure 3. Surface and interface recessions are shown in figure 3(a) and temperature histories at various locations within the material are shown in figure 3(b). It can be seen that the agreement is not good in either case. At any given time the calculated interface recession is greater than that indicated by the experimental data. The calculated char surface recession is too large initially but is too small after a test time

of about 90 seconds. The rapid increase in the experimental surface recession at about this time is most likely caused by mechanical removal of the char. The appearance of the char surface on the uninstrumented specimens shows a change at approximately 90 seconds from a fairly continuous surface structure to a columnar char structure. (Similar results were obtained in ref. 8.) The char which appears at the surface after about 90 seconds was formed when the heating rate at the interface was less than that present when the initial char surface was formed. It is postulated that the char formed at lower heating rates is less continuous than chars formed more quickly at higher heating rates and therefore a significant portion of the char is composed of loose particles which are swept away by the gas flow. This part of the char does not take part in the oxidation reaction and accounts for the difference between the analytical and experimental surface recession at the longer times since char removal by oxidation only was considered in the standard calculation. The surface recession is the same for all calculations since the temperature is sufficiently high in all cases to allow the oxidation reaction to be diffusion controlled; and thus the reaction no longer is a function of the surface temperature and not significantly influenced by variations in material properties.

The main differences between the calculated and experimental temperature histories shown in figure 3(b) can be explained by use of figure 3(a). The calculated interface depth is greater than that required for each thermocouple to pass by the interface at the specified pyrolysis temperature. Thus the calculated temperature rise at this location occurs too soon. It can be seen that at longer times the calculated temperature is too low. This effect is caused by the larger calculated char thickness as seen in figure 3(a). Because of the poor agreement between the experimental results and the standard calculation, the values of the material properties were varied about the values used in the standard calculation so that the effect of the variation could be determined. Since it is known how the standard calculation deviates from the experimental results, variations which are beneficial to better agreement could be determined.

Material Property Variations

Char conductivity.- The two variations in char conductivity considered were $k_c \propto T^4$ and $k_c \propto T$. The results of these calculations compared with the standard calculation are shown in figure 4.

The surface and interface recessions are shown in figure 4(a) for the three cases. The difference in the interface location for the three cases is very large and indicates that the thermal performance of the material is a strong function of the char conductivity. Analyses (not reported herein) also show this strong dependence of thermal performance on char conductivity and, in addition, predict an even stronger dependence in high-enthalpy

environments. As would be expected, the interface recession is greatest for the case which has the largest average conductivity.

The temperature histories of the first three thermocouple locations for the three conductivity variations are shown in figure 4(b). It can be seen that the differences in the temperature histories are somewhat greater than the differences in the interface locations. This phenomenon is due to the fact that the temperature gradients through the material are very severe, and therefore a relatively small change in position along the direction of heat flow will correspond to a large change in temperature. It can also be seen that differences in both interface location and temperature histories increase with time.

Specific heat of uncharred material.- In one case the value of the specific heat of the uncharred material increased linearly with temperature and doubled over the applicable temperature range, the initial value being the same as that for the standard calculation. In the other case, the specific heat was constant at twice the value of that of the standard calculation. The results of these calculations are shown in figure 5. As would be expected, the highest average specific heat produces the least interface recession and the lowest temperatures. Although the differences in the interface locations are not as great as those for the char conductivity variations (fig. 4(a)), it is apparent that changes in the specific heat of the uncharred material can have a significant effect on material performance. Again it can be seen that relatively small differences in the interface location are magnified in the temperature histories.

Uncharred material conductivity.- The two variations of the virgin material conductivity used were both constant. In one case the conductivity was one-half the constant value used in the standard calculation. In the other case it was twice the value used in the standard calculation. The results of these calculations are shown in figure 6.

The differences in the interface location for the three cases were negligible. This result is to be expected since the heat flow beyond the interface is comparatively small and thus conductivity changes in the virgin material should have little effect on interface location. However, the temperature histories show considerable variation during the time each thermocouple is in the uncharred material. The low conductivity produces a severe temperature gradient immediately behind the interface and hence most of the uncharred material remains at the initial temperature. This condition causes a delay in the initial temperature rise. However, the temperature rises very rapidly as the interface approaches. When the larger value for the conductivity is used, the temperature begins to rise sooner but does not rise as rapidly.

Heat of pyrolysis.- The values selected for the heat-of-pyrolysis variation were one-half and twice the standard value. The results of these calculations are shown in

8

figure 7. An examination of the figure shows that the thermal performance of the material is affected by a change in the heat of pyrolysis. When these results are compared with those of figure 5, it can be seen that doubling the heat of pyrolysis produces about one-half the change in interface recession as doubling the specific heat of the uncharred material. However, on a basis of the heat absorbed per pound of material, doubling the heat of pyrolysis has approximately the same effect on material performance as does doubling the specific heat of the uncharred material since only about half the material is affected by the heat of pyrolysis.

Temperature of pyrolysis.- In each case the temperature of pyrolysis varied over a certain range. This temperature range was obtained from an equation of the form

$$\dot{m} = Ae^{-B/T}$$

where $\dot{m}$ is the mass loss rate, A corresponds to a specific reaction rate constant, and B corresponds to an activation energy. The values of A and B used in the standard case were obtained from the data of reference 9 in which the temperature at which pyrolysis initiates and the temperature at which the reaction occurs very rapidly are given. The values of the constants which were used in the standard case produced a pyrolysis temperature range of 1100° R to 1300° R (611° K to 722° K).

The variations in the pyrolysis temperature range were obtained by changing the values of the constants A and B. In one case values were used which resulted in a pyrolysis temperature range of 1500° R to 1600° R (833° K to 889° K). In the other case, a range of 900° R to 1500° R (500° K to 833° K) was obtained. The results of these calculations are shown in figure 8.

It can be seen from figure 8 that neither raising the level nor increasing the range of the pyrolysis temperature produces any large change in the material performance. Increasing the range but keeping about the same average temperature of pyrolysis produces negligible changes in the interface recession (that is, produces essentially the same recession as does the standard) and very small changes in temperature histories within the material. Raising the average pyrolysis temperature by about 350° R (193° K) does cause small changes in the interface location and in the temperature histories, but, in general, does not affect the performance of the material greatly. Only one temperature curve corresponding to a depth of 0.14 inch (0.36 cm) is shown since up to this depth, the interface recession curves for the three cases considered are essentially the same. Therefore, as would be expected, the temperatures calculated for this location are the same for each case.

The relatively small effect of variation of pyrolysis temperature on material performance results from the severe temperature gradients on each side of the interface;

these temperature gradients cause relatively large temperature differences at the interface to produce only small changes in interface location.

Specific heat of gases of pyrolysis.- The specific heat of the gases of pyrolysis increased linearly with temperature for the standard calculation. The variations of this property which were used were a constant value (equal to the value for the uncharred material) and a value which increased with temperature up to about 2000° R (1100° K) and then decreased. The choice of specific heat used in the standard calculation was somewhat arbitrary. The specific heat was made to increase as the temperature increases to account for the heat absorbed as the gases decompose because of the temperature rise they experience as they pass through the char layer. As the gases decompose, they decrease in molecular weight; therefore, the specific heat of the gaseous mixture should increase. The increase-decrease specific-heat variation was obtained from reference 3 (which was not available when the standard values were chosen). This specific heat was calculated from a plot of the enthalpy of nylon-phenolic pyrolysis gases as a function of temperature. Although this investigation involves a different material, it is felt that the heat absorption of the pyrolysis gases should not be substantially different for the two materials. The results of the calculations with different pyrolysis gas specific heats are shown in figure 9.

An examination of figure 9 shows that the performance of the material is a strong function of the value of the specific heat of the pyrolysis gases. This result was not unexpected since reference 3 indicates that the heat absorbed by the gases of pyrolysis as they pass through the char layer is a primary mechanism in the heat-accommodation characteristics of a charring ablator.

Final Case

After considering the comparisons of the results of the various calculations and the comparison of the standard calculation with the experimental results, further calculations were made with various material property inputs to obtain closer agreement between the experimental and calculated results. A comparison between the experimental results and the best analytical results obtained is shown in figure 10. As mentioned previously, in the standard calculation the char was assumed to be removed by oxidation only and it can be seen from figure 3 that this method did not produce very satisfactory results. It is possible, however, to put into the program a char mass loss rate which is a function of time. In this way it is possible to match the experimental surface recession exactly. The experimental mass loss rate as a function of time was used in the final calculation instead of the mass loss rate calculated from oxidation considerations. This procedure was used because one cannot expect to calculate correct internal temperatures and hence determine representative values for material properties if the surface is not in the right location.

10

It can be seen that the results from the final calculation agree much more favorably with the experimental results than do the results of the standard calculation. However, except for the front surface location, there is still some difference between experimental and calculated results. There is little doubt that the difference in interface recession is due, in part, to the error involved in determining the actual interface location experimentally. The analytical program assumes that pyrolysis takes place in a plane. In an actual material, pyrolysis occurs over a zone. (See fig. 11.) The boundaries of this zone are difficult to determine and the location in the zone where the assumed plane interface should be placed is not known at present. Therefore, the experimental interface recessions shown in figures 3, 10, and 12 are subject to some error.

It can be seen from figure 10(b) that for a given time, the difference between the temperature indicated by a particular thermocouple and the corresponding calculated temperature is relatively large. However, because of the very steep slopes of the temperature curves, the temperature differences correspond to relatively small shifts in time or position. The differences between the experimental and calculated temperatures are undoubtedly caused in part by the uncertainty in the locations of the thermocouple junctions. It is difficult to determine the exact location of a thermocouple junction embedded in a material and, as mentioned previously, small changes in position can lead to relatively large changes in temperature. For example, some unpublished experimental data have shown that a temperature difference of as much as 700° R (411° K) can exist over a distance equal to one diameter of the size thermocouple wire used in this study. Also, because of the heat-sink effect of the thermocouple inside the ablation material, the thermocouple may indicate a temperature which is less than the temperature which would exist at the point if the thermocouple were not present. In view of these uncertainties in the experimental data as well as the uncertainties in the material properties, the agreement between the analytical and experimental results is good.

The material property values used in the final case are given in table II. The three properties which differ from those used in the standard case are the thermal conductivity of the char, the specific heat of the gases of pyrolysis, and the specific heat of the uncharred material. All other material properties are the same as those for the standard case.

The thermal conductivity of the char used in the final case is $k \propto T^4$. This variation gives a relatively lower conductivity at low temperatures and a higher conductivity at high temperatures. This variation tends to delay the temperature response at a specific location in the material, but then causes the temperature to increase more rapidly after the initial delay. Figure 3 shows that an effect of this kind would be conducive to better agreement.

The specific heat of the gases of pyrolysis used in the final case was the variation obtained from reference 3 from a plot of the enthalpy of nylon-phenolic pyrolysis gases as a function of temperature.

The effect of this variation is similar to the effect caused by the final char conductivity used. A large heat absorption near the interface occurs which delays the temperature rise at this point. The subsequent decrease in the specific heat of the pyrolysis gases at higher temperatures allows the temperature to increase more rapidly than would a specific heat which continues to increase.

The specific heat of the uncharred material used in the final case is $c_p \propto T$. This variation produces the best approximation to the shape of the experimental temperature curves when the thermocouple is still in the uncharred material. If the value of specific heat which is twice the standard value is used, the calculated temperature histories for the deeper thermocouples are lower than the experimental temperatures when each temperature shows its initial rise, and then cross over the experimental temperature histories. Recent work on errors in temperature measurement with thermocouples in ablation materials shows that the actual temperature at an undisturbed point in the material is always as high and usually higher than the temperature obtained with a thermocouple at the point. Thus a case which shows a lower calculated temperature was considered unacceptable.

Similar comparisons between the final case and the experimental results obtained from tests in 100-percent nitrogen are shown in figure 12. No surface recession curve is shown since the experimental tests showed that no surface recession occurred in this atmosphere. It can be seen that the difference between experimental and calculated results are approximately the same as that for the 3-percent oxygen atmospheres.

The performance of an ablation material is extremely sensitive to surface location. Therefore, although the test environments were very similar for the two test conditions, the differences in surface location should produce a markedly different response through the material. Thus, although it is not claimed that the material property values used in the final case are unique, the comparatively good agreement in two test conditions (which should produce a very different material response) lends some validity to using the results obtained in this investigation for predictions of material performance in different environments.

CONCLUDING REMARKS

A series of calculations was made to determine the effect of varying certain material property values on the performance of a charring ablator in a heating environment. The effect of changing the level or the temperature dependence of these properties on the

performance of the material as evidenced by surface and interface recessions and internal temperatures is shown. The calculated results are compared with experimental results to determine whether the material property values used in the calculations are representative of those of the ablation material.

The results of this investigation show that with the variations in material properties used, the thermal conductivity of the char layer and specific heat of the gases of pyrolysis affect the thermal response of the material to a greater extent than any of the other properties considered. The temperatures in the uncharred material are affected considerably by changes in the conductivity of the uncharred material. However, these changes do not significantly affect the recession rates or the temperatures within the char layer. Large changes in both the specific heat of the uncharred material and the heat of pyrolysis affect the performance of the material to some extent. However, doubling the value of the specific heat produces approximately twice the change in interface recession as doubling the heat of pyrolysis. The temperature of pyrolysis is seen to be a relatively unimportant parameter since raising the average or increasing the range of the pyrolysis temperature has little effect on internal temperatures and negligible effect on the interface recession.

· Analytical results were obtained which are in good agreement with experimental results when the uncertainties in the experimental results as well as in the material properties are considered. The differences between experimental and analytical results are approximately the same in the simulated flight environment (5-percent oxygen, 95-percent nitrogen) as in the 100-percent nitrogen environment.

Langley Research Center,
        National Aeronautics and Space Administration,
                Langley Station, Hampton, Va., March 14, 1966.

REFERENCES

1. Brooks, William A., Jr.; Wadlin, Kenneth R.; Swann, Robert T.; and Peters, Roger W.: An Evaluation of Thermal Protection for Apollo. NASA TM X-613, 1961.

2. Swann, Robert T.; Pittman, Claud M.; and Smith, James C., Jr.: One-Dimensional Numerical Analysis of the Transient Response of Thermal Protection Systems. NASA TN D-2976, 1965.

3. Kratsch, K. M.; Hearne, L. F.; and McChesney, H. R.: Thermal Performance of Heat Shield Composites During Planetary Entry. Presented at AIAA-NASA National Meeting (Palo Alto, Calif.), Sept. 30 - Oct. 1, 1963.

4. Wilson, R. Gale: Thermophysical Properties of Six Charring Ablators From 140° to 700° K and Two Chars From 800° to 3000° K. NASA TN D-2991, 1965.

5. Mechtly, E. A.: The International System of Units — Physical Constants and Conversion Factors. NASA SP-7012, 1964.

6. Chapman, Andrew J.: An Experimental Investigation of Three Types of Thermal Protection Material at Moderate Heating Rates and High Total Heat Loads. NASA TN D-1814, 1963.

7. Swann, Robert T.; Dow, Marvin B.; and Tompkins, Stephen S.: Analysis of the Effects of Environmental Conditions on the Performance of Charring Ablators. AIAA Entry Technology Conference, CP-9, Am. Inst. Aeron. Astronaut., Oct. 1964, pp. 259-269.

8. Dow, Marvin B.; and Swann, Robert T.: Determination of Effects of Oxidation on Performance of Charring Ablators. NASA TR R-196, 1964.

9. Neĭman, M. B.; Kovarskaya, B. M.; Golubenkova, L. I.; Strizhkova, A. S.; Levantovskaya, I. I.; and Akutin, M. S.: The Thermal Degradation of Some Epoxy Resins. J. Polymer Sci., vol. 56, 1962, pp. 383-389.

TABLE I.- ENVIRONMENTAL CONDITIONS AND TEST PROCEDURES

Heating rate		Enthalpy		Stream composition	Number of specimens tested		Test time, sec	
$Btu/ft^2\text{-}sec$	MW/m^2	Btu/lb	MJ/kg		Uninstrumented	Instrumented	Uninstrumented specimens	Instrumented specimens
160	1.8	3000	7.0	5-percent oxygen, 95-percent nitrogen	6	1	30, 60, 90, 120, 150, 180	Until back surface temperature increased 300° R (167° K)
140	1.6	3000	7.0	100-percent nitrogen	6	1		

TABLE II.- MATERIAL PROPERTY VARIATIONS

Uncharred material properties

	Temperature		Standard		Variation I		Variation II		Final	
	°R	°K	k = Constant		k = Constant		k = Constant		k = Constant	
Thermal conductivity			Btu/ft-sec °R	W/m-°K	Btu/ft-sec °R	W/m-°K	Btu/ft-sec °R	W/m-°K	Btu/ft-sec °R	W/m-°K
			2.0×10^{-5}	0.12	1.0×10^{-5}	0.06	4.0×10^{-5}	0.25	2.0×10^{-5}	0.12
			C_p = Constant		$C_p \propto T$		C_p = Constant		$C_p \propto T$	
			Btu/lb-°R	J/kg-°K	Btu/lb-°R	J/kg-°K	Btu/lb-°R	J/kg-°K	Btu/lb-°R	J/kg-°K
Specific heat	500	278	0.32	1300	0.32	1300	0.64	2700	0.32	1300
	800	444			.46	1900			.46	1900
	1000	556			.55	2300			.55	2300
	2000	667			.64	2700			.64	2700
Density			lb/ft³	kg/m³	lb/ft³	kg/m³	lb/ft³	kg/m³	lb/ft³	kg/m³
			57.5	92.0	57.5	92.0	57.5	92.0	57.5	92.0

Charred material properties

	Temperature		Standard		Variation I		Variation II		Final	
	°R	°K	$k = AT^3 - BT + C$		$k \propto T$		$k \propto T^4$		$k \propto T^4$	
			Btu/ft-sec-°R	W/m-°K	Btu/ft-sec-°R	W/m-°K	Btu/ft-sec-°R	W/m-°K	Btu/ft-sec-°R	W/m-°K
Thermal conductivity	500	278	0.5×10^{-5}	0.03	1.0×10^{-5}	0.06	0.5×10^{-5}	0.03	0.5×10^{-5}	0.03
	1000	556	.9	.06	2.0	.12	.5	.03	.5	.03
	1500	833	2.0	.12	3.0	.19	2.5	.16	2.5	.16
	2000	1111	5.6	.35	4.0	.25	8.0	.50	8.0	.50
	2500	1389	12	.75	5.0	.31	20	1.2	20	1.2
	3000	1667	20	1.2	6.0	.37	41	2.6	41	2.6
	3500	1945	33	2.1	7.0	.44	75	4.7	75	4.7
	4000	2222	49	3.1	8.0	.50	128	8.0	128	8.0
			Btu/lb-°R	J/kg-°K	Btu/lb-°R	J/kg-°K	Btu/lb-°R	J/kg-°K	Btu/lb-°R	J/kg-°K
Specific heat	500	278	0.23	960	0.23	960	0.23	960	0.23	960
	1000	556	.30	1300	.30	1300	.30	1300	.30	1300
	1500	833	.35	1500	.35	1500	.35	1500	.35	1500
	2000	1111	.37	1500	.37	1500	.37	1500	.37	1500
	2500	1389	.38	1600	.38	1600	.38	1600	.38	1600
	3000	1667	.39	1600	.39	1600	.39	1600	.39	1600
	3500	1945	.40	1700	.40	1700	.40	1700	.40	1700
	4000	2222	.41	1700	.41	1700	.41	1700	.41	1700
Density			lb/ft³	kg/m³	lb/ft³	kg/m³	lb/ft³	kg/m³	lb/ft³	kg/m³
			25	401	25	401	25	401	25	401
Emissivity			0.9	0.9	0.9	0.9	0.9	0.9	0.9	0.9

Pyrolysis characteristics

|	Temperature		Standard		Variation I		Variation II		Final			
	°R	°K	$\overline{C}_p \propto T$		$\overline{C}_p \propto T^3$		$\overline{C}_p$ = Constant		Temperature		$\overline{C}_p = f(T)$	
			Btu/lb-°R	J/kg-°K	Btu/lb-°R	J/kg-°K	Btu/lb-°R	J/kg-°K	°R	°K	Btu/lb-°R	J/kg-°K
Specific heat of gases of pyrolysis	500	278	0.13	540	0.02	80	0.32	133	500	278	0.30	1 300
	1000	556	.25	1000	.18	750			1000	556	.78	3 300
	1500	833	.38	1600	.62	2 600			1250	695	1.2	5 000
	2000	1111	.50	2100	1.5	6 300			1500	833	2.1	8 800
	3000	1667	.75	3100	5.0	21 000			1665	925	4.0	17 000
	4000	2222	1.0	4200	11.0	46 000			2000	1111	2.1	8 800
									2500	1389	1.1	4 600
									3000	1667	.75	3 100
									3500	1945	.98	4 100
Heat of pyrolysis			Btu/lb	MJ/kg	Btu/lb	MJ/kg	Btu/lb	MJ/kg	Btu/lb		MJ/kg	
			250	0.58	125	0.29	500	1.16	250		0.58	
Temperature of pyrolysis			°R	°K	°R	°K	°R	°K	°R		°K	
			1100 to 1300	611 to 722	900 to 1600	500 to 889	1500 to 1600	833 to 889	1100 to 1300		611 to 722	
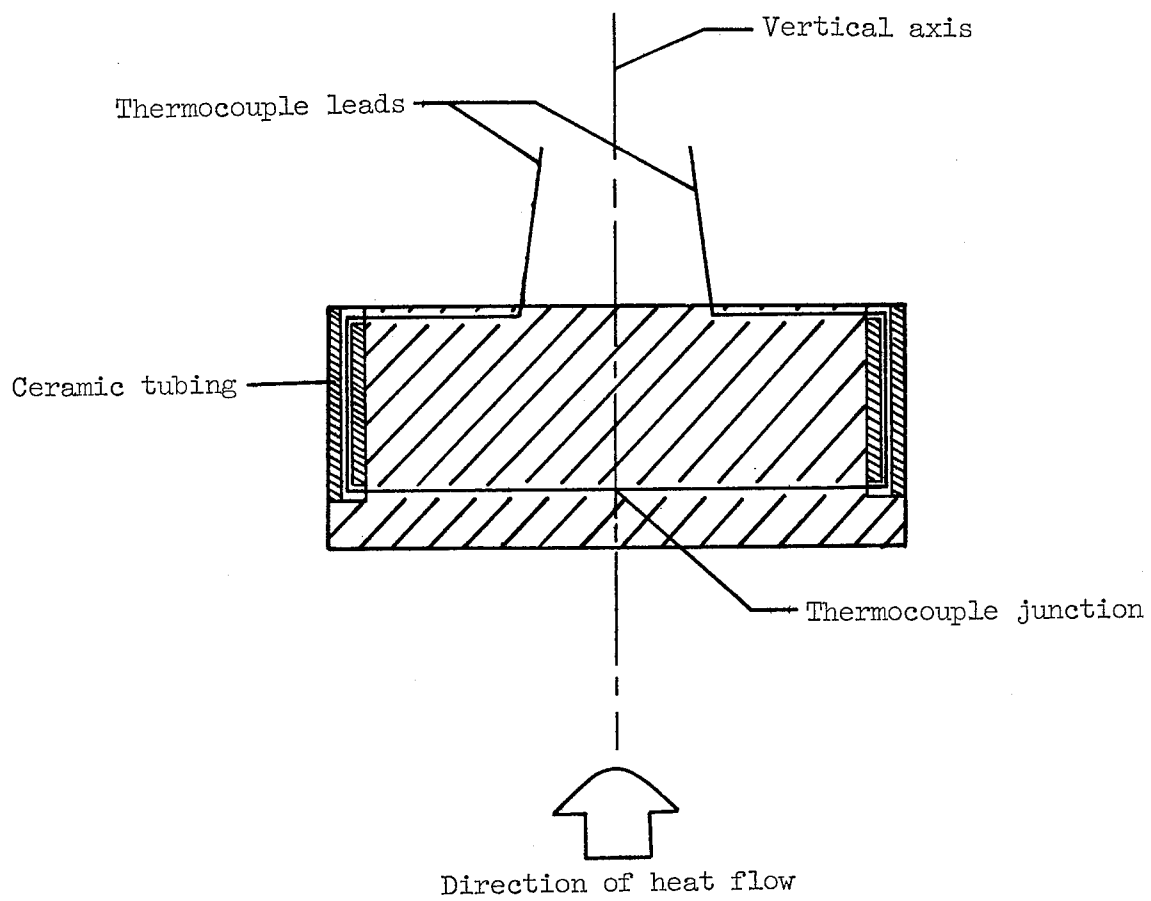
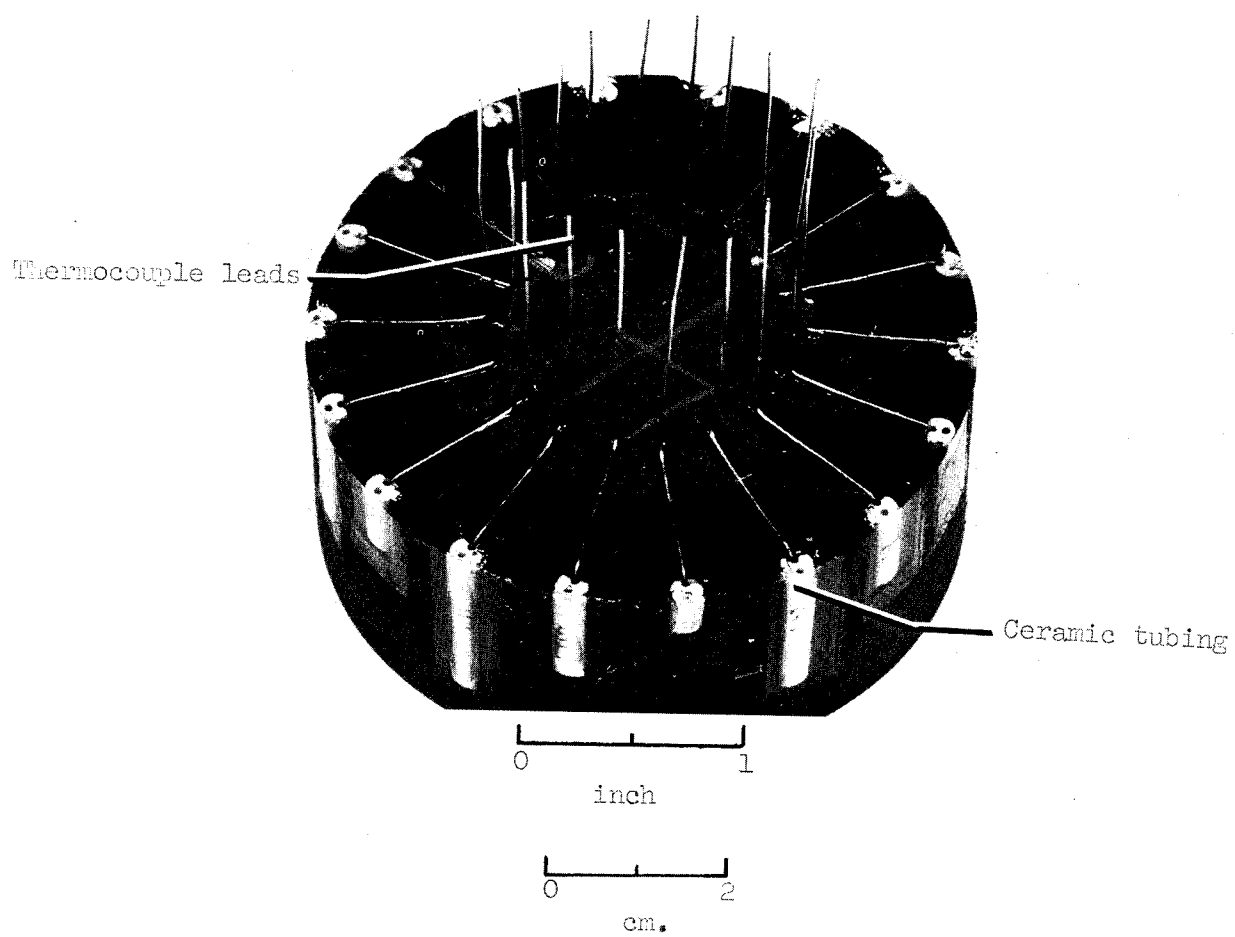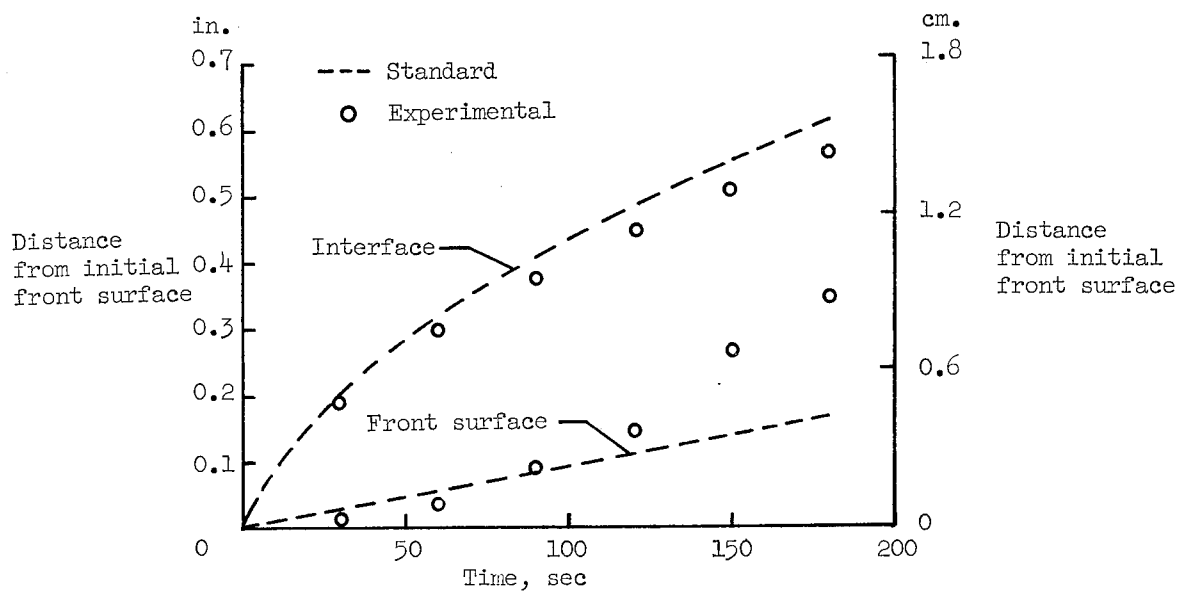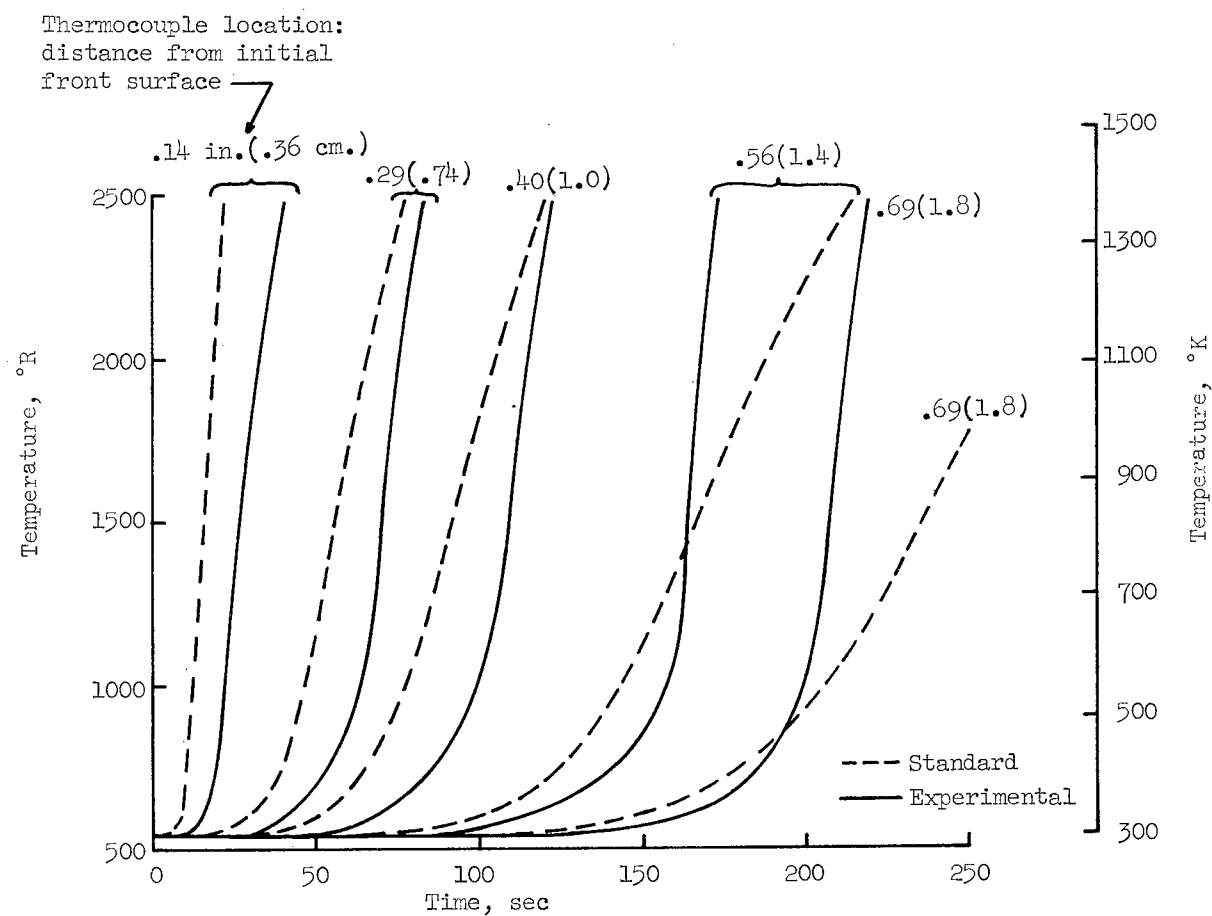Figure 1.- Typical thermocouple installation for instrumented specimen.

Figure 2.- Instrumented specimen prior to attachment of mounting ring.   L-62-8157.1
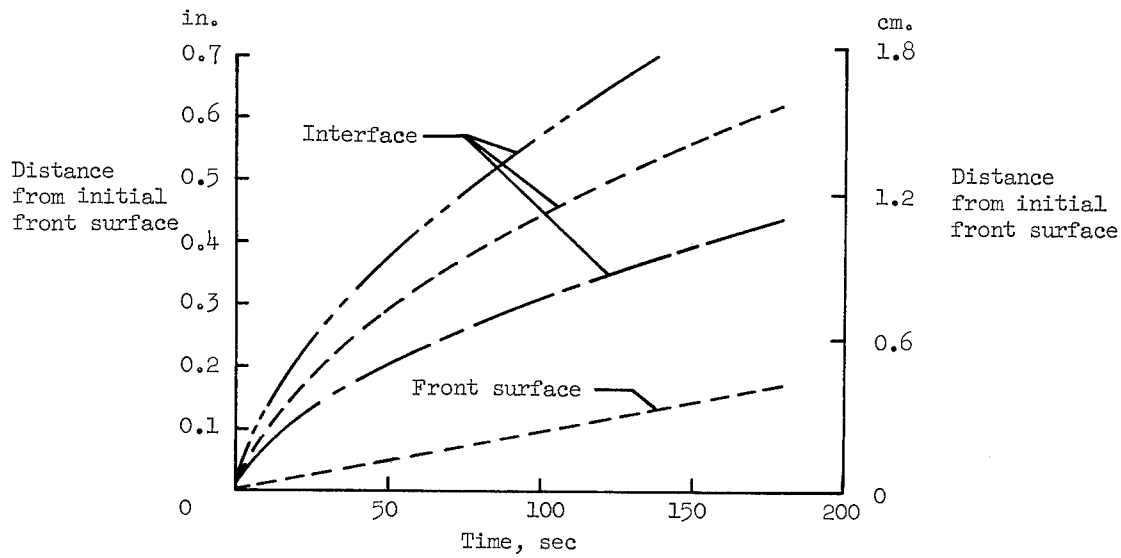
18

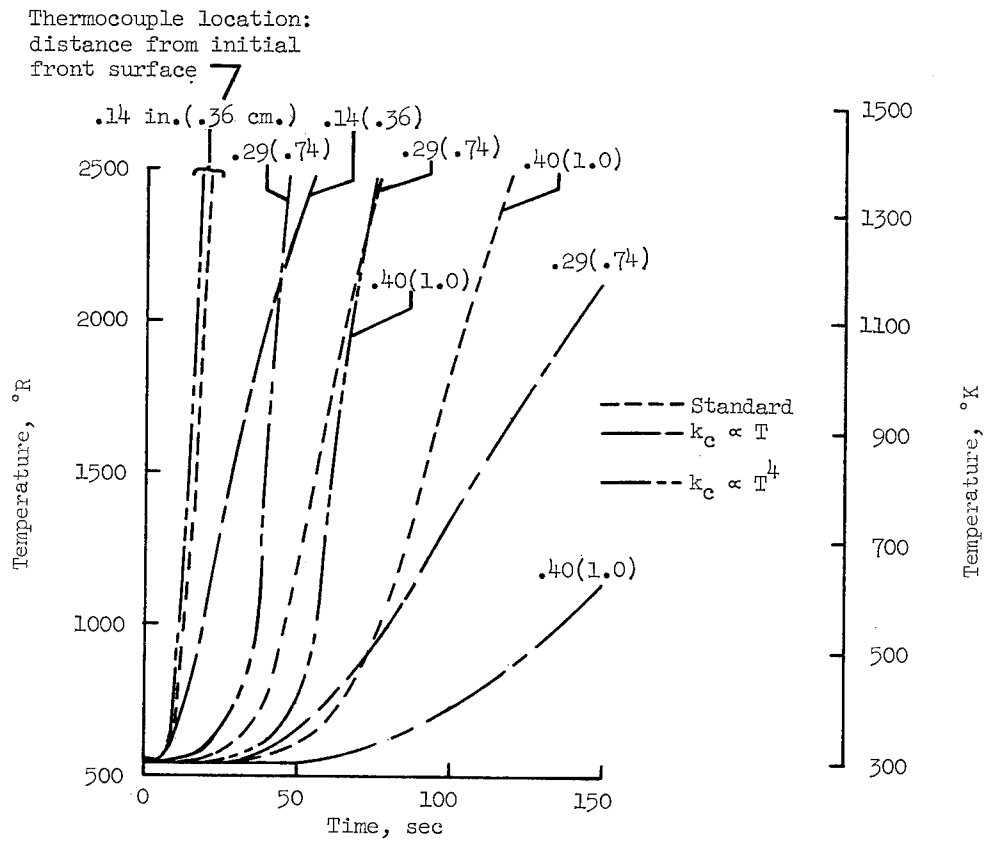(a) Surface and interface recession.

(b) Temperature histories.

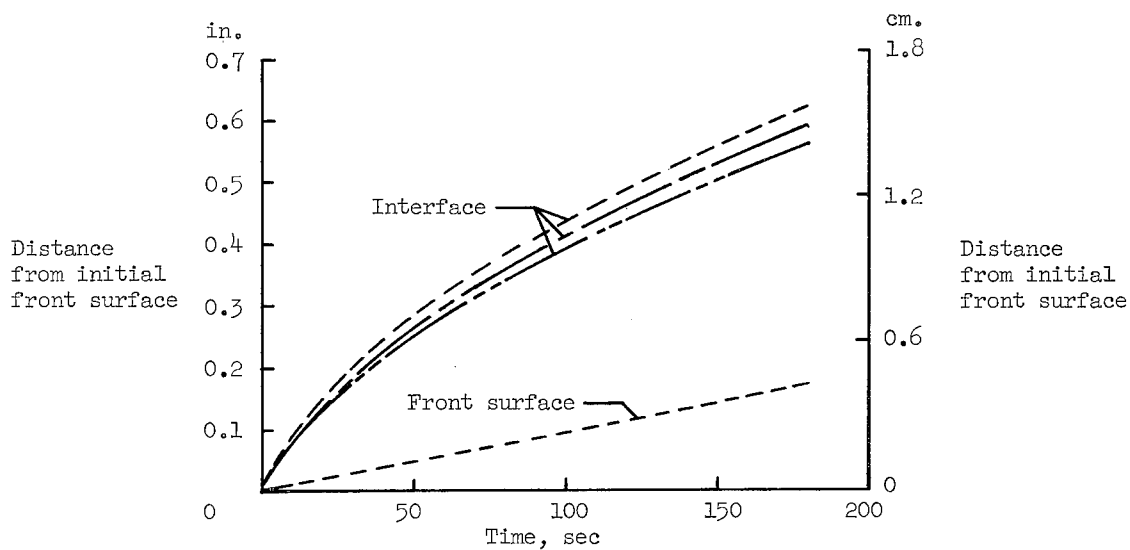Figure 3.- Comparison of standard calculation and experimental results.
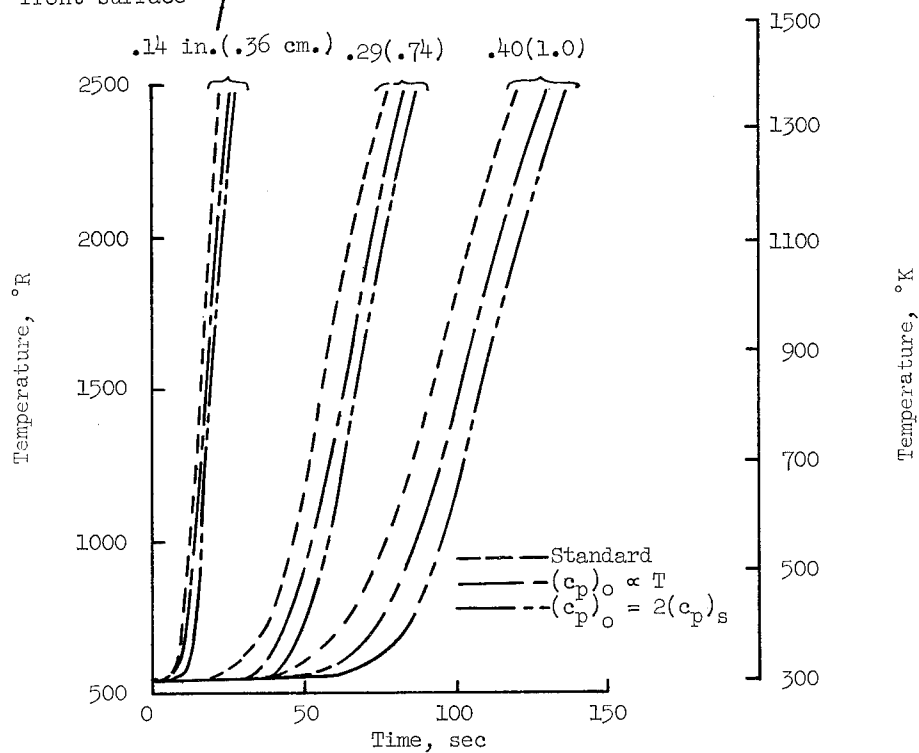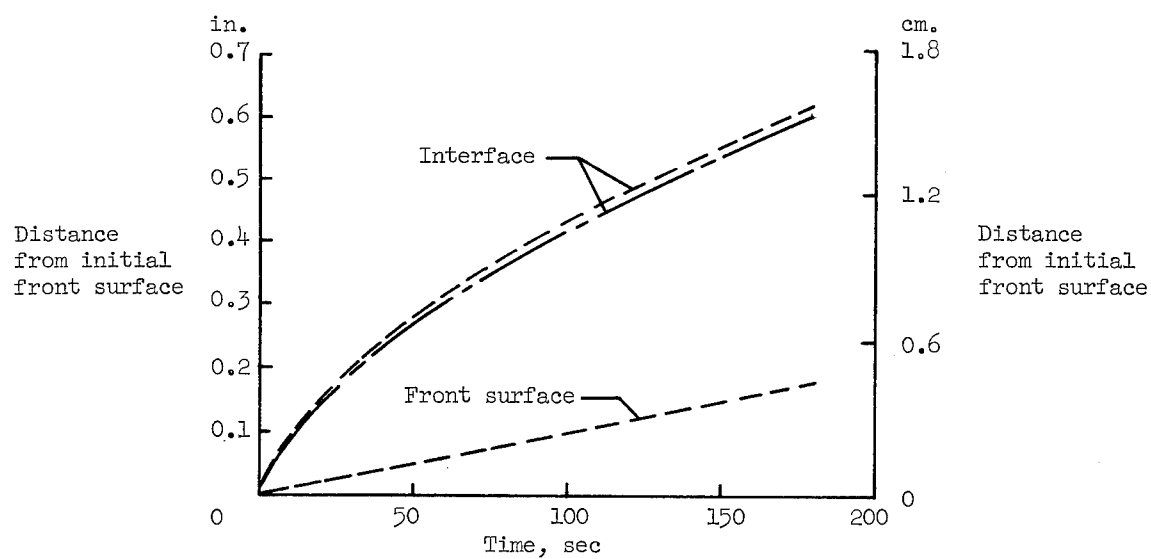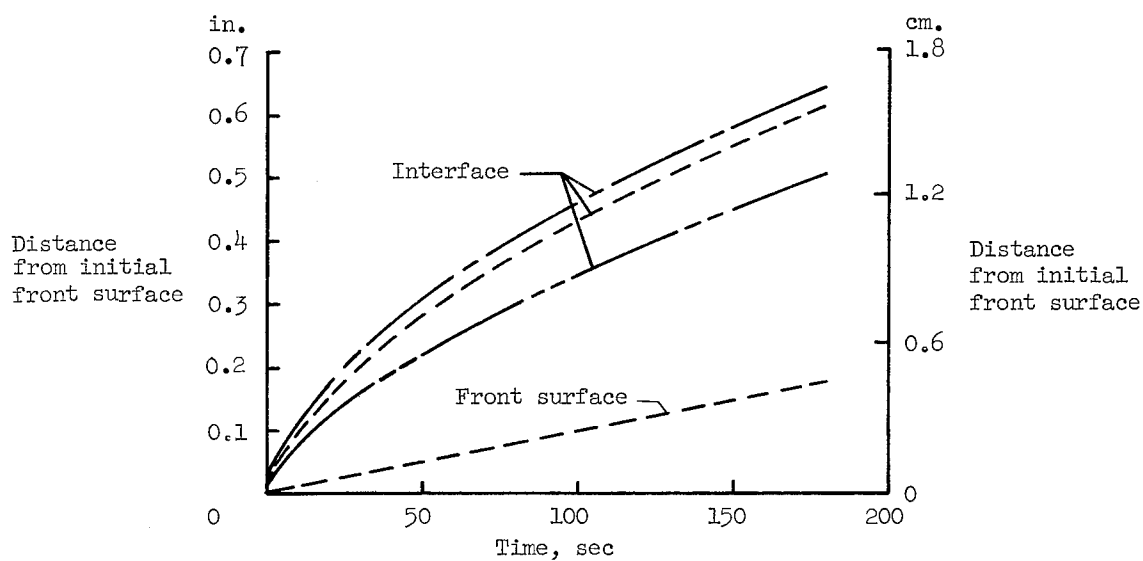
19

(a) Surface and interface recession.

(b) Temperature histories.

Figure 4.- Comparison of results for char conductivity variation.
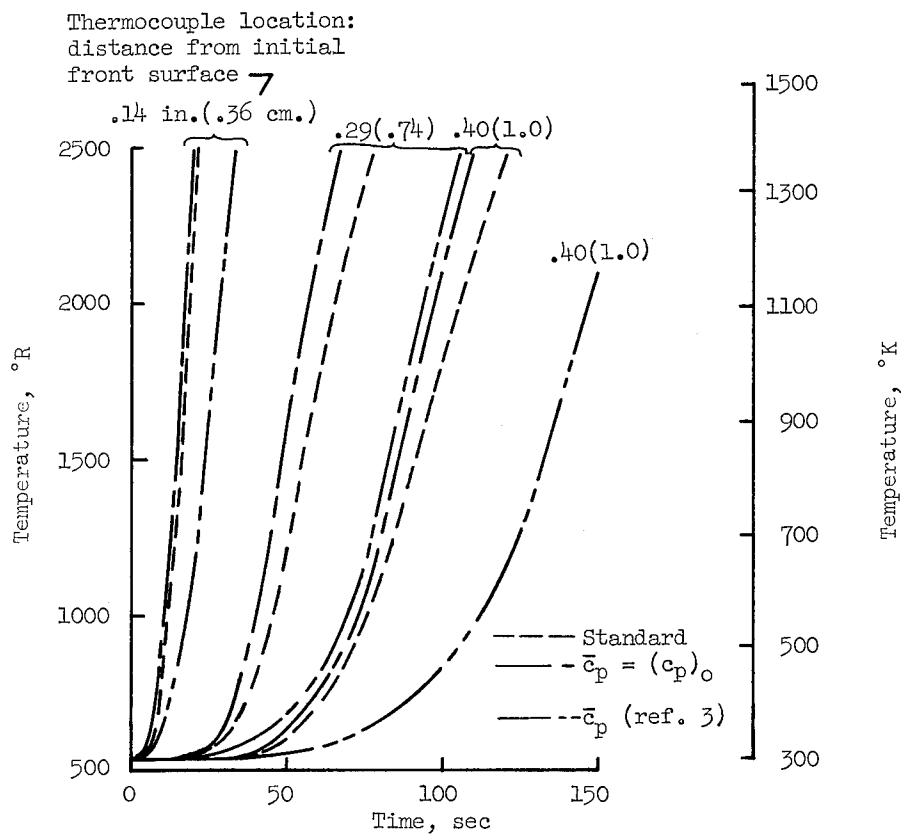
20

(a) Surface and interface recession.

(b) Temperature histories.

Figure 5.- Comparison of results for uncharred material specific-heat variation.
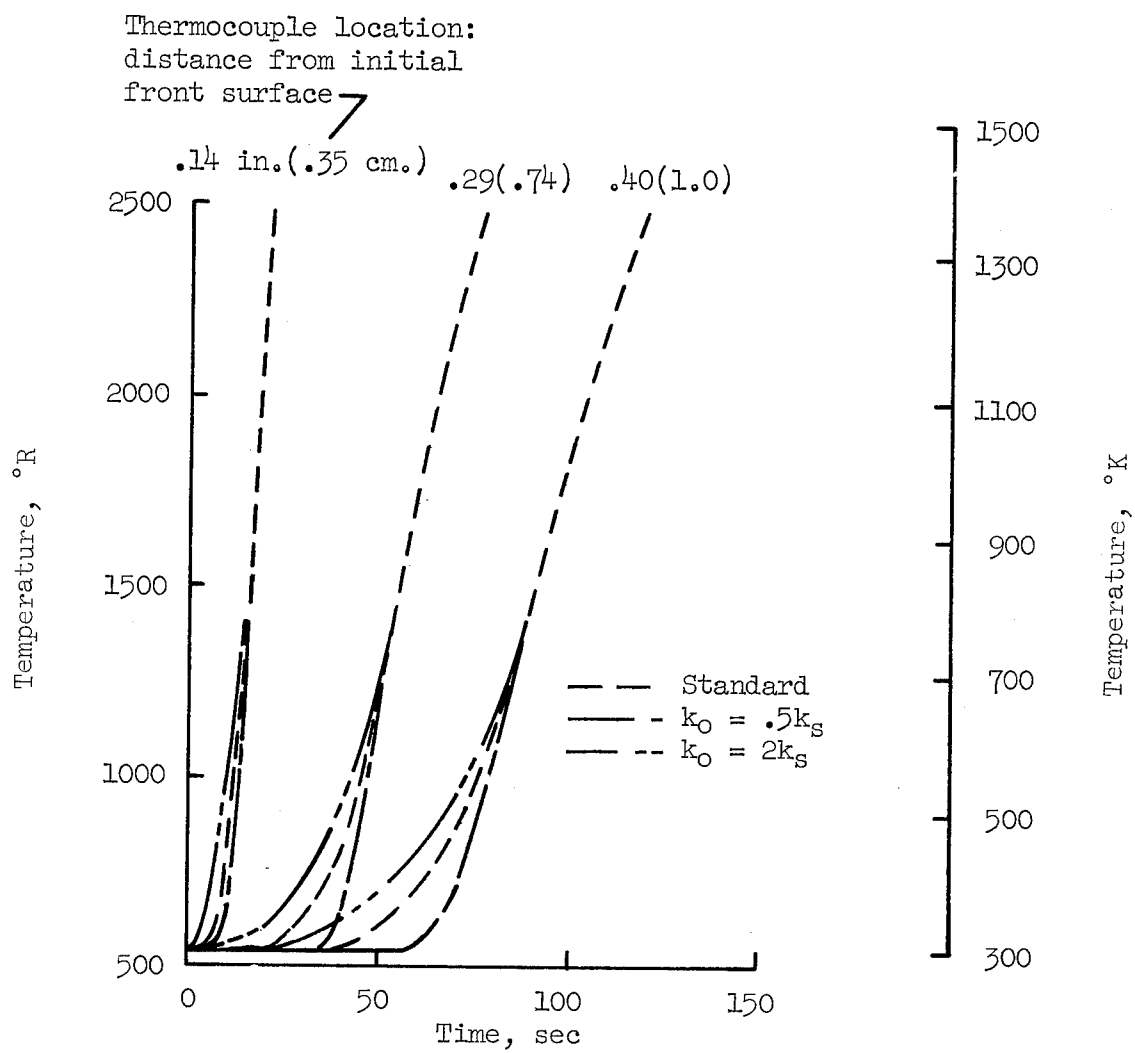
Figure 6.- Comparison of temperature histories for uncharred material conductivity variation.
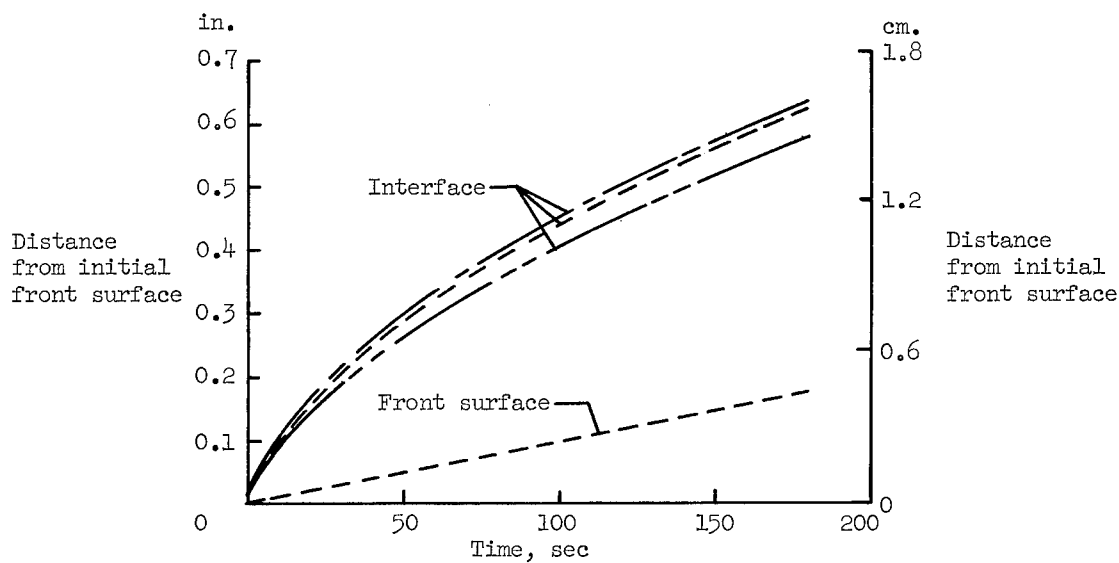
(a) Surface and interface recession.
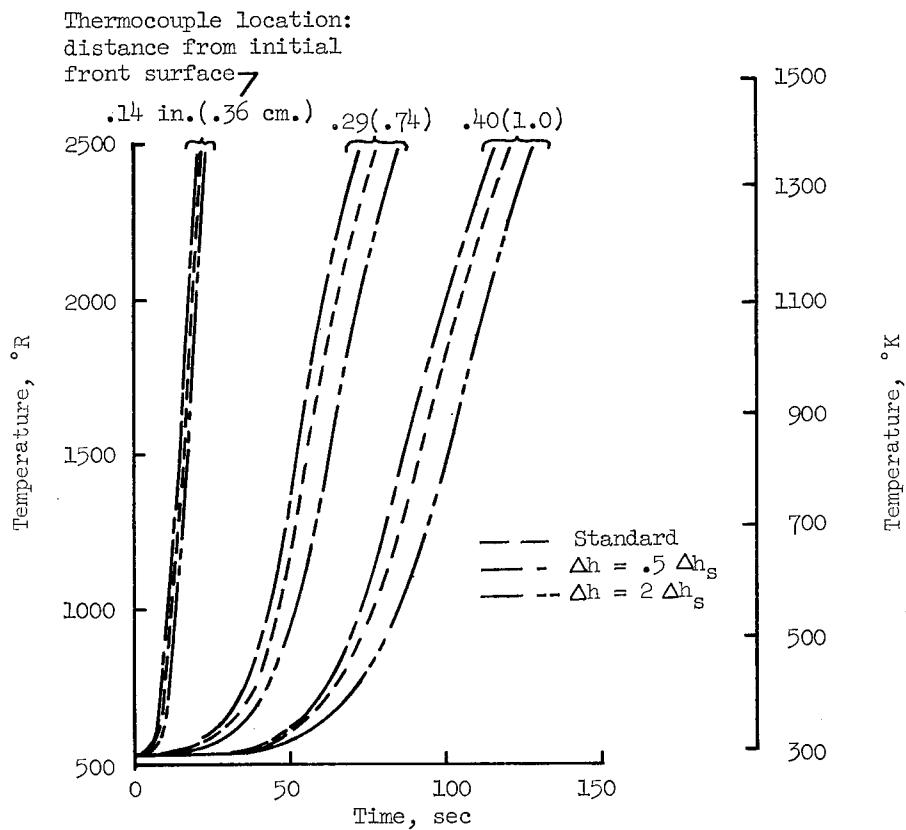
(b) Temperature histories.

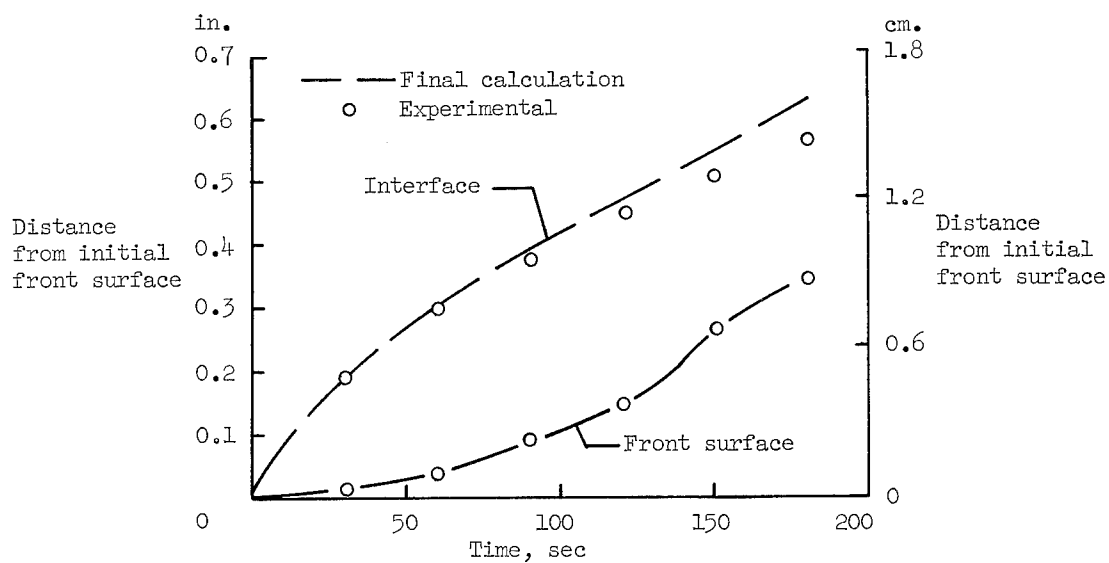Figure 7.- Comparison of results for heat-of-pyrolysis variation.

23

(a) Surface and interface recession.

(b) Temperature histories.

Figure 8.- Comparison of results for temperature of pyrolysis variation.

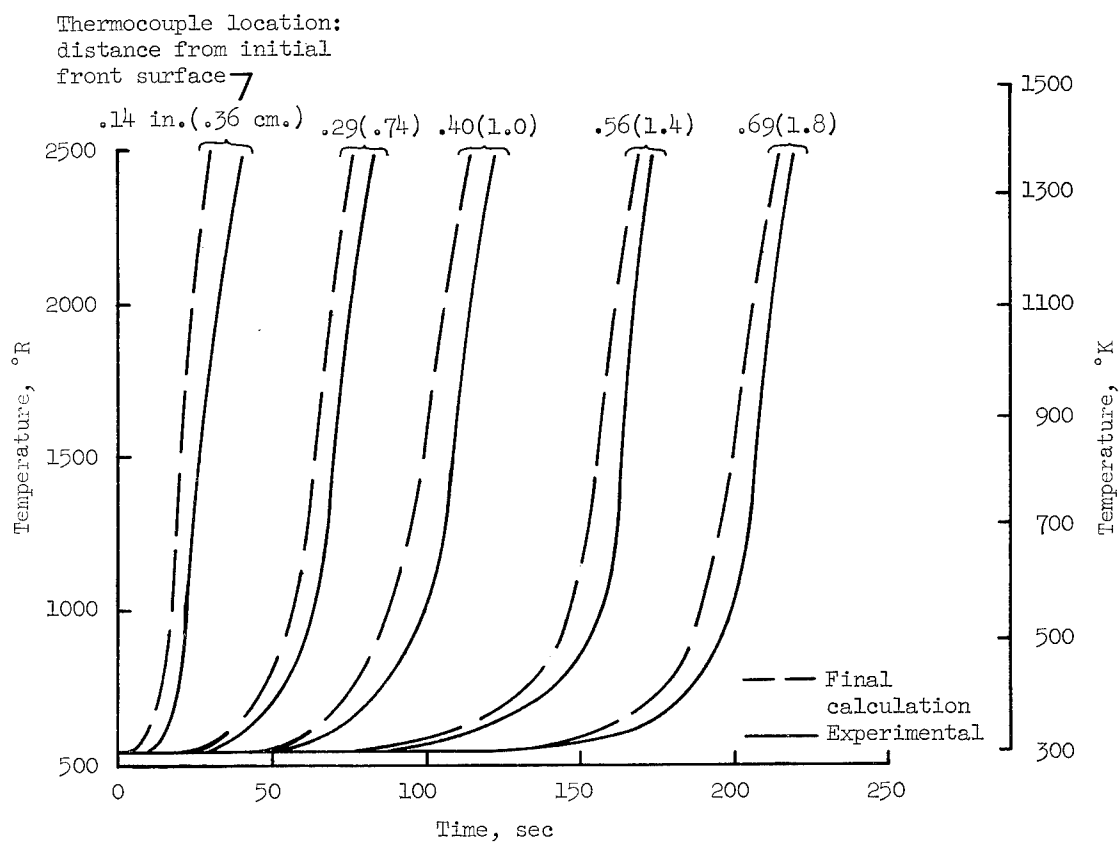(a) Surface and interface recession.

(b) Temperature histories.

Figure 9.- Comparison of results for pyrolysis-gas specific-heat variation.

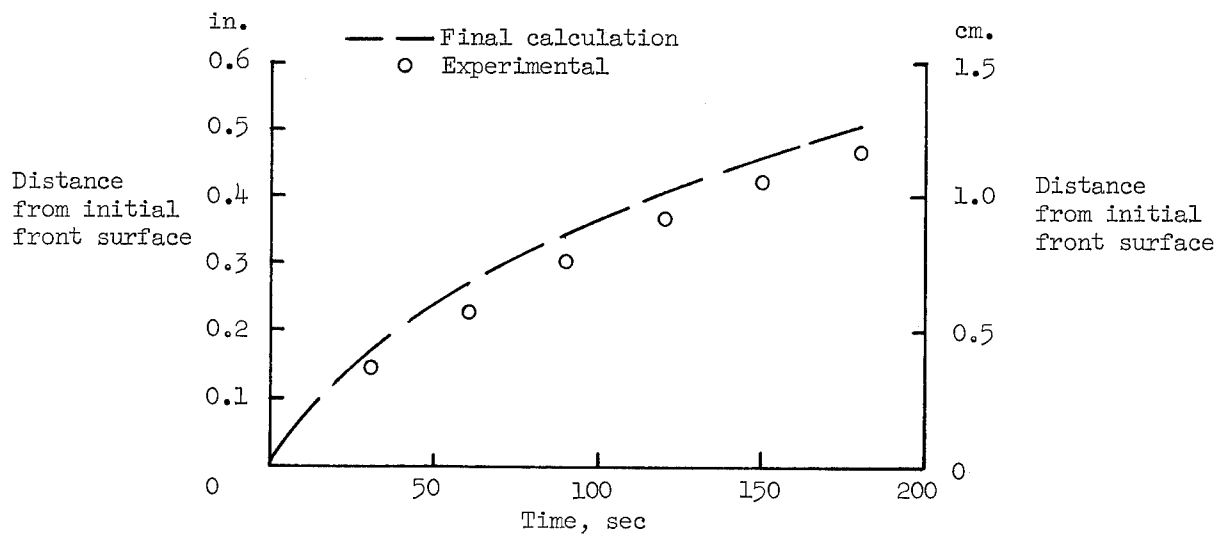(a) Surface and interface recession.

(b) Temperature histories.

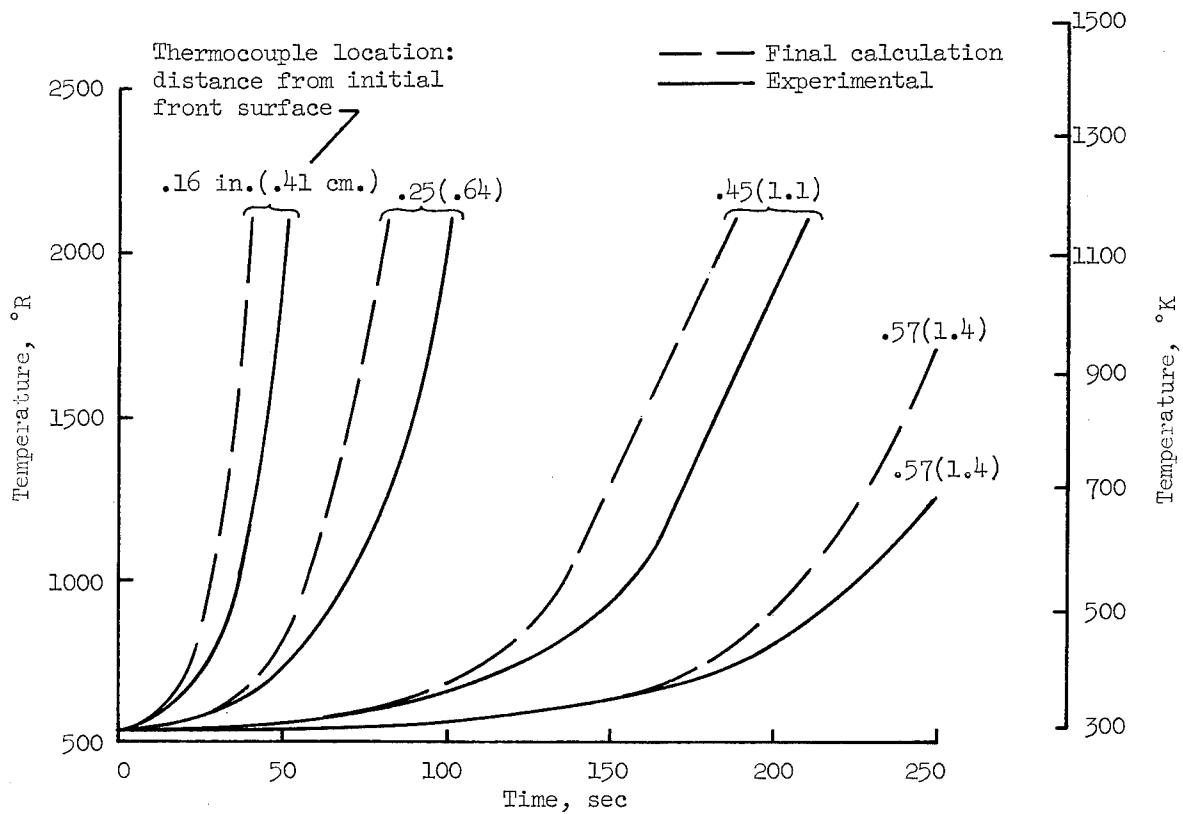Figure 10.- Comparison of final calculation and experimental results.

Char layer

Pyrolysis zone

Uncharred material

L-65-7202.1

Figure 11.- Enlarged view of sectioned specimen after testing.

0

0.1

in.

0

2

mm.

(a) Interface recession.

(b) Temperature histories.

Figure 12.- Comparison of final calculation and experimental results in nitrogen atmosphere.